Scaling with MgO thickness of the proximity exchange field in a Fe/MgO/Si contact

R. Jansen,[1] A. Spiesser,[1] Y. Fujita,[1,2,3] H. Saito,[1] K. Hamaya,[2] and S. Yuasa[1]

[1]*Research Center for Emerging Computing Technologies, National Institute of Advanced Industrial Science and Technology (AIST), Tsukuba, Ibaraki, 305-8568, Japan*

[2]*Center for Spintronics Research Network, Graduate School of Engineering Science, Osaka University, Toyonaka 560-8531, Japan*

[3]*Research Center for Magnetic and Spintronic Materials, National Institute for Materials Science (NIMS), Tsukuba, Ibaraki 305-0047, Japan*

(Received 20 September 2022; revised 12 December 2022; accepted 3 January 2023; published 12 January 2023)

The scaling of the proximity exchange field, which ferromagnetic Fe exerts on the spin accumulation at the MgO/Si interface of Fe/MgO/Si tunnel contacts, was investigated using the inverted Hanle effect. Data as a function of the applied bias voltage shows that the exchange field varies with bias in the same way as the square of the tunnel spin polarization (TSP). The decay of the exchange field with increasing MgO thickness t_{MgO} is rather weak and nonexponential, which we argue to be related to the improved epitaxial quality of the MgO, and the, consequently, improved spin-filtering properties at larger MgO thickness. Using the TSP data to correct for this yields an exponential decay of the exchange field with t_{MgO} with a decay length of $\lambda = -0.42$ nm. Comparing this to the decay length for the tunnel conductance ($\lambda = -0.21$ nm) suggests that the exchange interaction is dominated by two-step tunneling processes.

DOI: 10.1103/PhysRevB.107.024411

I. INTRODUCTION

The exchange interaction that exists in a ferromagnetic material is known to extend into an adjacent nonmagnetic material across the interface between the two materials [1–3]. This proximity exchange interaction induces magnetism in the nonmagnetic material, but only in the first few layers close to the interface, as the proximity exchange field is short range and decays exponentially as a function of the distance from the boundary [1–3]. The interest in this phenomenon has recently been revived [4–9] in studies of two-dimensional (2D) materials, such as graphene and van der Waals heterostructures [3,10–14] because the entire 2D layer is within the range of the proximity exchange field. The presence of strong proximity-induced magnetic exchange fields with values up to 1 T or larger has been observed in graphene and other monolayer materials in direct contact with a ferromagnet [4–6].

Exchange across a tunnel barrier between two ferromagnets was discussed by Slonczewski [15] and was observed in crystalline MgO-based magnetic tunnel junctions [16–19]. Since the exchange interaction is attenuated by the tunnel insulator [15], the tunneling-mediated proximity exchange between a ferromagnet (FM) and a nonmagnetic (NM) material is expected to be rather weak and the induced magnetization in the NM material is small. The strong exponential decay of the proximity exchange interaction was confirmed by monitoring the decay of spin pumping between a ferromagnetic insulator and a Pt NM layer as a function of the thickness of an insulating barrier [20], noting that the spin pumping is mediated by the exchange interaction. In Co/CdMgTe/CdTe structures with a 10-nm CdMgTe barrier [21], the small proximity-induced exchange splitting in the NM was detected directly using spin-flip Raman scattering. Interestingly, even if the exchange fields across a tunnel barrier are not very large, small fields can be used [5,9,22] to induce spin precession of a spin accumulation in a NM material. If the exchange field is perpendicular to the spins (the Hanle effect configuration [23,24]), the required magnetic fields are in the 1–10-mT range if the spin-relaxation time is on the order of a few nanoseconds. Indeed, in Fe/MgO/Si tunnel contacts, the proximity-induced exchange field that extends across the MgO tunnel barrier was shown to modify the spin precession of the spin accumulation localized at the MgO/Si interface [25,26]. The exchange field produces distinct features in the so-called inverted Hanle effect [27], including exchange-induced shifts of the inverted Hanle curves, hysteresis, and discontinuities at the coercive field of the ferromagnet at which the exchange field is reversed [25,26]. The proximity exchange field was found to be locked antiparallel to the magnetization of the ferromagnet, depends on the bias voltage across the tunnel contact, and persists up to room temperature [26]. The Fe/MgO/Si contacts with a crystalline MgO barrier exhibit [28–30] a very large tunnel spin polarization (TSP), thus, producing large spin accumulations up to 10 meV. This makes these structures ideally suited to study proximity exchange across a tunnel barrier in detail.

Here we set out to examine the scaling of the exchange field with the thickness of the MgO tunnel insulator in Fe/MgO/Si contacts. Although one can expect that the exchange field decays exponentially as the MgO thickness is increased, we contemplated that it is essential to take into account that the epitaxial quality of the MgO, and, consequently, the tunnel spin polarization, are not constant when the thickness of the MgO barrier is changed [30]. Indeed, we find that the observed decay of the exchange field with MgO thickness is rather weak and nonexponential because the decay is countered by the improved spin-filtering properties of the MgO at larger thickness. A means to correct for this is

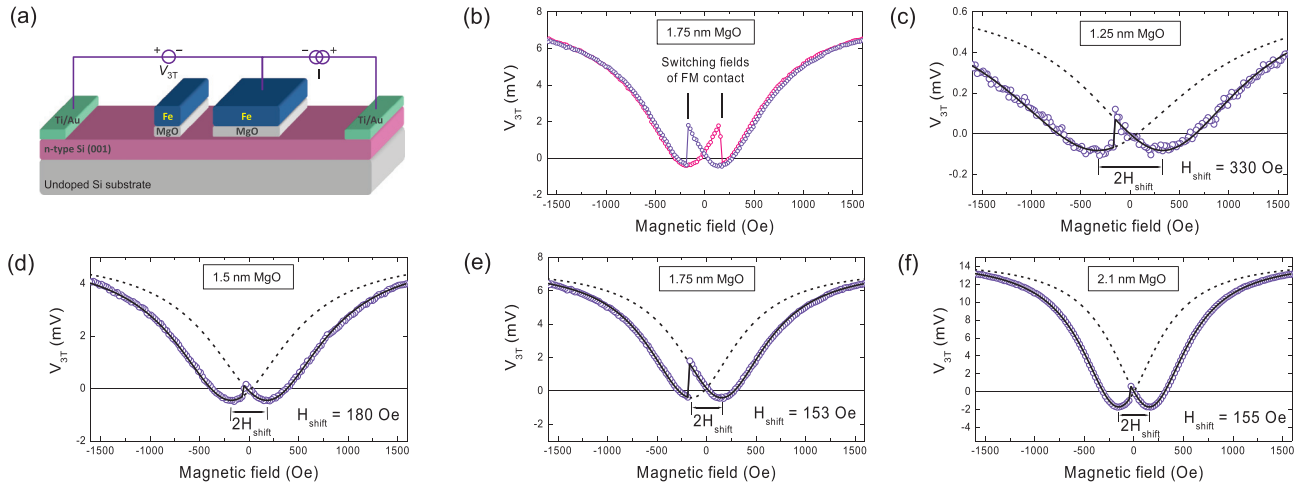

FIG. 1. (a) Device layout and three-terminal measurement geometry. (b) Example of the inverted Hanle curve for a Fe/MgO/Si contact of an O-type device with a 1.75-nm MgO barrier. The magnetic field was swept from − to + (pink symbols) or in the opposite direction (blue symbols). The discontinuities in the curves occur at the switching fields of the 1-μm wide ferromagnetic contact, as indicated. (c)–(f) Measured inverted Hanle curves (symbols) for O-type devices with different MgO thickness, as indicated, for one field sweep direction only (+ to −). The solid lines are fits. The dashed lines visualize that the fits are constructed from two inverted Hanle curves that are shifted left and right along the magnetic-field axis, respectively. The minima of the two curves are separated by two times the shift field $H_{\rm shift}$ as indicated. Ferromagnetic contacts of different widths were used, and so the discontinuities at the switching fields of the contacts do not occur at the same magnetic field for all devices. All data were obtained at 10 K and the three-terminal offset voltage of +840 ± 2 mV was subtracted from all the data.

suggested by data as a function of the applied bias voltage, which shows that the exchange field varies with bias in the same way as the square of the tunnel spin polarization. It is shown that the corrected proximity exchange field decays exponentially with a decay length of −0.42 nm, corresponding to a decay by about an order of magnitude per extra nanometer of MgO. We will compare this to the decay of the tunnel conductance and discuss the implications.

II. EXPERIMENT

The experiments were performed on crystalline Fe/MgO/Si tunnel contacts [Fig. 1(a)] grown by molecular beam epitaxy onto Si(001) substrates containing a 70-nm thick *n*-type Si channel (phosphorous doped, carrier density 2.7×10^{19} cm^{-3} at 10 K). Most of the data were obtained on a set of devices that was fabricated by optical lithography, referred to as the O-type devices. The thickness $t_{\rm MgO}$ of the MgO layer varies from 1.25 to 2.3 nm and the ferromagnetic contacts are 20-μm long and 1–5-μm wide. These O-type devices have previously [30] been used in nonlocal spin-transport experiments to determine the dependence of the TSP on the thickness of the MgO. Some of the experiments reported here were performed on another device that was fabricated by e-beam lithography, referred to as the E-type device. The MgO tunnel barrier is 1.8-nm thick and the Fe/MgO contacts employed here are 40-μm long and 0.4-μm wide. The E-type device has previously been used not only in nonocal spin-transport experiments [28,29], but also in our previous report on the observation of the proximity exchange field [25]. For details of the device growth, fabrication and characterization, we refer the reader to those previous publications [25,28–30].

In order to determine the proximity exchange field from the Fe, we use a single Fe/MgO/Si contact and two nonmagnetic reference contacts [Fig. 1(a)] in a three-terminal (3T) measurement configuration [31,32]. A charge current I is sent from the Fe/MgO contact to one of the Ti/Au reference contacts, and the voltage V_{3T} is measured between the same Fe/MgO contact and the other Ti/Au reference contact. The spin current across the tunnel contact induces a spin accumulation of the mobile electrons in the Si channel, but it also induces a spin accumulation of electrons that are trapped in the MgO/Si interface region either in interface states or in the depletion region that is a few nanometers wide for heavily doped Si. Because the spin accumulation due to mobile electrons spreads out into the Si channel on a length scale of the spin-diffusion length (2.4 μm at 10 K), the effect of the short-range exchange field from the Fe is rather weak, and we have so far not detected any sign of an exchange field in nonocal spin-transport measurements on these Si-based devices. However, the electrons localized at the MgO/Si interface are very close to the Fe and experience a significant exchange field (of up to several 100 Oe), which produces characteristic changes in the spin precession of the localized spin accumulation as previously shown [25]. The exchange field can, therefore, be extracted from the inverted Hanle curves [27] in a 3T measurement geometry with the applied magnetic field collinear with the in-plane oriented magnetization of the ferromagnetic electrode.

III. RESULTS

A. Determination of the exchange field

As an example, the inverted Hanle curve for an O-type device with a 1.75-nm MgO barrier is shown in Fig. 1(b). The

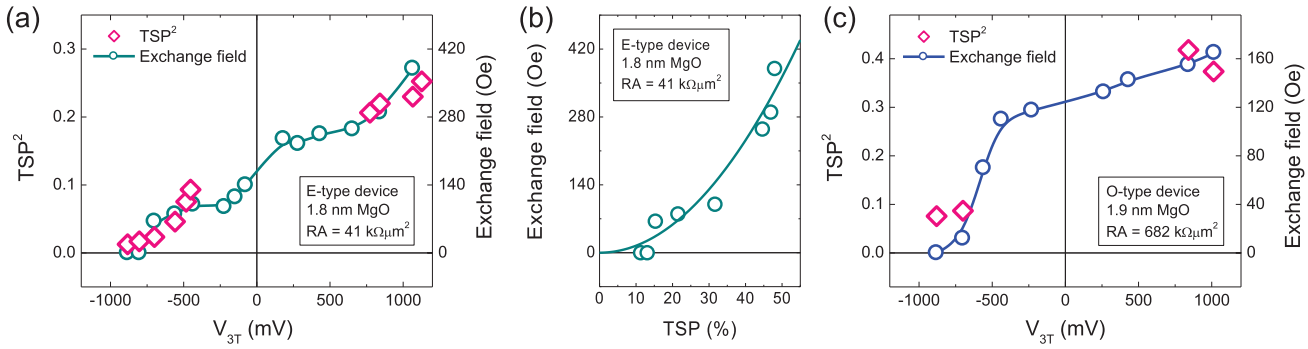

FIG. 2. Scaling of the exchange field with bias voltage across the Fe/MgO/Si tunnel contact. (a) Exchange field (green circles, right axis, data taken from Ref. [25]) and TSP^2 (red diamonds, left axis) as a function of the applied bias voltage for the E-type device with a 1.8-nm MgO tunnel barrier with a resistance-area (RA) product of 41 $k\Omega\mu m^2$ at a bias voltage of +840 mV. (b) Exchange field versus TSP as extracted from the data in (a) for the E-type device. The solid line is a fit for a quadratic dependence on the TSP. (c) Exchange field (blue circles, right axis) and TSP^2 (red diamonds, left axis) as a function of the applied bias voltage for the O-type device with a 1.9-nm MgO tunnel barrier with a RA product of 682 $k\Omega\,\mu m^2$ at a voltage of +840 mV. All data were obtained at 10 K.

characteristic features [25] of the proximity exchange field can be recognized. The curves exhibit hysteresis, there are discontinuities at the switching fields of the Fe electrode at which the exchange field changes sign, and, most importantly, the minimum of the inverted Hanle curve is shifted away from zero field either to the left or to the right, depending on the direction of the magnetic-field sweep. These features are consistent with a proximity exchange field that is collinear with the magnetization of the Fe electrode and locked antiparallel to the Fe magnetization, as observed previously for the E-type device [25].

Examples of inverted Hanle curves for selected O-type devices with different MgO thicknesses are shown in Figs. 1(c)–1(f). The proximity exchange field is present for all these devices. The solid lines represent fits of the inverted Hanle curves. As visualized by the dashed lines, the fits are composed of two identical Lorentzian functions that are shifted along the magnetic field axis in the + and − directions, respectively, depending on the direction of the exchange field. When the Fe magnetization points in the + direction, the exchange field is negative. Adding this to the external magnetic field shifts the curve in the + direction. When the Fe magnetization points in the − direction, the exchange field is positive, and the shift is in the − direction. As the applied magnetic field is swept from + to −, the Fe magnetization is reversed at its coercive field. This causes the exchange field to abruptly change sign as well, thus, creating a discontinuous transition between the two Lorentzian curves. The width of the Lorentian curves is set by the magnitude of the magnetostatic fields due to roughness of the ferromagnetic film [27], and by the effective spin lifetime, which varies from 50 to 125 ps depending on the MgO thickness. The distance between the minima of the two Lorentzian curves is equal to two times the shift field $H_{\rm shift}$, the latter being equal to the proximity exchange field $H_{\rm exch}$ safe for the minus sign. In the remainder of this article, we will quote only positive values of the exchange field, keeping in mind that the exchange field is locked antiparallel to the Fe magnetization [25].

Although from this data the dependence of the exchange field on the MgO thickness can be obtained, we note that it has previously been reported [30] that for these O-type devices, the TSP of the magnetic tunnel contacts increases with increasing MgO thickness. For the most part, this is because the crystalline quality of the MgO layer improves for thicker MgO barriers. We expect that the exchange field also depends on the crystalline quality of the tunnel insulator because the exchange interaction across a tunnel insulator is mediated by spin-polarized states and their decay into the tunnel barrier [15]. We will, therefore, first determine the correlation between the value of the TSP and the magnitude of the exchange field for a fixed thickness of the MgO barrier.

B. Exchange field and the TSP

The correlation between the exchange field and the TSP becomes evident when examining how those two quantities depend on the tunnel bias voltage across the Fe/MgO/Si contact. Figure 2(a) displays data for the E-type device. The data for the exchange field (green symbols) as a function of V_{3T} was taken from Ref. [25]. In order to evaluate the correlation with the TSP, which was previously not examined, we added to Fig. 2(a) the newly obtained data for the square of the TSP (pink symbols). The TSP was extracted from nonlocal spin-transport measurements using the previously established procedures and parameters [28–30] with the tunnel bias voltage varied by changing the tunnel current across the injector Fe/MgO/Si contact. As can be seen, for positive voltage (electrons tunneling from the Fe into the Si) the TSP is large (about 50%) and also the exchange field is largest (about 400 Oe). On the other hand, for negative voltage the TSP is much smaller and goes down to almost zero, and so does the exchange field. This suggests that there indeed is a correlation between the TSP and the exchange field. This becomes more evident if for each bias voltage, we take the values of the TSP and the exchange field, and plot the latter two quantities against each other [Fig. 2(b)]. We observe that the exchange field increases as a function of the TSP, and that the relation is quadratic, i.e., the exchange field is proportional to the square of the TSP as indicated by the solid line. Additional data for one of the O-type devices [Fig. 2(c)] reveals the same trend, i.e., the exchange field and the TSP are large at positive bias, and both are significantly reduced at large negative voltage.

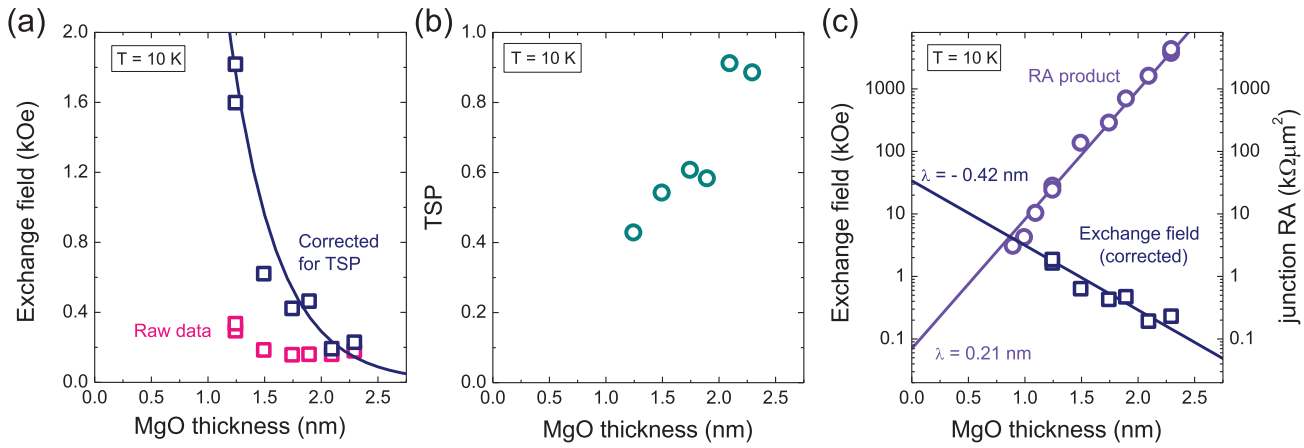

FIG. 3. Scaling of the exchange field with MgO thickness. (a) Exchange field as a function of the MgO thickness for the O-type devices. The red symbols are the raw data for the exchange field as extracted from the inverted Hanle curves. The dark blue symbols are obtained after correcting for the fact that the TSP varies with MgO thickness, as shown in panel (b). The solid line in (a) is a fit assuming an exponential decay. (c) Exchange field as a function of the MgO thickness, plotted on a logarithmic scale. For easy comparison, we also included the previously obtained data for the junction RA product, taken from Ref. [30]. The solid lines are fits assuming exponential dependencies, $\exp(t_{\mathrm{MgO}}/\lambda)$ with the values of λ as indicated. All data was obtained at 10 K at a bias voltage of $+840 \pm 2$ mV.

Note that whereas the exchange field can readily be obtained for low bias from the large inverted Hanle effect (3T measurement), the extraction of the TSP from nonlocal spin-transport data becomes increasingly inaccurate at low current through the magnetic injector contact. Therefore, TSP data is only available at larger bias. Also note that the growth procedure for the MgO tunnel barrier was different for the E-type and the O-type devices so that the resistance-area product of the E-type device is not the same as that of the O-type devices with a comparable MgO thickness.

Although some kind of correlation between the exchange field and the TSP may have been expected as both quantities depend on the transmission of the spin-polarized electrons across the tunnel oxide, to the best of our knowledge, the expected functional relationship has never been predicted for a FM/insulator/NM junction. We, therefore, proceed by first writing the TSP as $\mathrm{TSP}_0 \times F(V, t_{\mathrm{MgO}})$, with the function $F(V, t_{\mathrm{MgO}})$ describing the dependence of the TSP on the bias voltage V and barrier thickness t_{MgO}. We then propose the following empirical relation for the exchange field:

$$H_{\mathrm{exch}} \propto F(V, t_{\mathrm{MgO}})^2 \exp\left(\frac{t_{\mathrm{MgO}}}{\lambda}\right). \tag{1}$$

The parameter λ is a length scale that determines the exponential decay as a function of the MgO thickness as described below (with $\lambda < 0$). Because $F(V, t_{\mathrm{MgO}}) = \mathrm{TSP}/\mathrm{TSP}_0$, Eq. (1) produces a quadratic relation between the exchange field and the TSP at a given t_{MgO}, consistent with the data in Fig. 2. Moreover, it also suggests that a purely exponential decay with t_{MgO} may be obtained if we plot the measured exchange field divided by TSP^2 as a function of t_{MgO}.

C. Exchange field and MgO thickness

We can now discuss the variation of the exchange field with tunnel barrier thickness. Figure 3(a) displays the corresponding data, extracted from fits of the inverted Hanle curves, such as shown in Figs. 1(b)–1(e). The red symbols are the raw data for the exchange field. For 1.25 nm of MgO, H_{exch} is largest (290–330 Oe). It decays to about 150 Oe at around 1.75 nm of MgO. However, for thicker MgO barriers up to 2.1 nm, the exchange field does no longer decay and, in fact, it even increases slightly to about 175 Oe for the largest MgO thickness (2.3 nm). The dependence of the exchange field on the MgO thickness is, thus, rather weak and does not follow the naively expected exponential decay. We attribute this to the fact that the TSP depends on the thickness of the MgO barrier and increases significantly for thicker MgO barriers [see Fig. 3(b)], reaching values of around 90%. The intrinsic exponential decay of the exchange field is, thus, compensated by the better spin-filtering properties of the thicker MgO barriers. We can correct the data for the exchange field by dividing the raw data by TSP^2 since according to Eq. (1) we have $H_{\mathrm{exch}}/\mathrm{TSP}^2 \propto \exp(t_{\mathrm{MgO}}/\lambda)$. The corrected data for the exchange field [blue symbols in Fig. 3(a)] exhibits a much stronger decay with MgO thickness. In fact, it can be described reasonably well by an exponential decay (solid line) according to $H_0 \exp(t_{\mathrm{MgO}}/\lambda)$ with $\lambda = -0.42$ nm and $H_0 = 34$ kOe, noting that there is some scatter of the data around a perfectly exponential decay. Figure 3(c) displays the corrected exchange field as well as the junction RA product on a logarithmic scale, confirming the exponential dependence on t_{MgO} for both. A notable feature is that the value of λ for the RA product (0.21 nm) is half of that for the exchange field (except for the different sign).

The value of 0.42 nm we extracted for the decay length of the exchange field is comparable to the decay lengths obtained from spin pumping across tunnel insulators [20], which yielded values between 0.16 and 0.74 nm for different barrier materials (Sr_2GaTaO_6, $SrTiO_3$, Sr_2CrNbO_6, and amorphous Si). With regard to the observed scaling of the exchange field with the tunnel barrier thickness, a comparison with available theory is warranted. First-principles calculations of the proximity exchange interaction in specific FM/insulator/NM structures have been reported, for instance, with graphene

or transition-metal dichalcogenides as the NM and hexagonal boron nitride as the tunnel insulator [33,34]. However, a generic analytical description of proximity exchange in a FM/insulator/NM junction with a current-induced spin accumulation is not available to the best of our knowledge. Some guidance may be obtained from the theory of exchange coupling across a tunnel barrier between *two* ferromagnetic metals [15] presented by Slonczewski. Using a free-electron description of spin-dependent tunneling, he derived that both the tunnel conductance and the exchange coupling energy are dominated by an exponential decay term $\exp(-2\kappa\, d)$ with d as the thickness of the tunnel barrier (t_{MgO} in our description), and the factor -2κ (equivalent to $1/\lambda$ in our description) determines the decay of the wave functions in the tunnel barrier for direct elastic tunneling. This does not agree with our result, since we find that the decay lengths for the exchange field and the tunnel conductance (inverse of the RA product) are different.

A clue comes from the factor of (minus) 2 difference between the values of λ that we extracted from the data for the exchange field (-0.42 nm) and the RA product (0.21 nm). It is well known that defects and/or impurity states in tunnel junctions give rise to additional current due to resonant or two-step tunneling processes. In experiments [35] on tunneling through amorphous Si it was convincingly established that whereas the conductance for direct tunneling is governed by an exponential decay factor of $\exp(-2\kappa\, d)$, the decay factor for two-step tunneling via localized states is given by $\exp(-\kappa\, d)$. The decay length, thus, differs by exactly a factor of 2 with the conductance for two-step tunneling decaying more slowly with barrier thickness. This feature is corroborated by theory of resonant tunneling [35–37]. A second notable point is that first-principles calculations [38] of the exchange coupling energy in Fe/MgO/Fe junctions show that resonant tunneling via localized states not only contributes to the exchange coupling, but that it provides a much larger coupling strength than direct tunneling. Considering a superposition of elastic tunneling and two-step tunneling, we propose that a possible scenario to explain our observations is that: (i) the elastic tunneling dominates the overall tunnel conductance [which yields RA product $\propto \exp(2\,\kappa\, d)$], and (ii) the two-step tunneling dominates the exchange coupling [which yields $H_{\mathrm{exch}} \propto \exp(-\,\kappa\, d)$]. This would produce a factor of (minus) two difference in the value of λ for the exchange field and the RA product as we observe. This scenario requires that the contribution of two-step processes to the tunnel conductance is relatively small, but the exchange interaction produced by a two-step process must be much larger than for a direct tunneling process. This mechanism may also have been relevant in spin-pumping experiments across insulators [20], which yielded the slowest decay (largest decay length of 0.74 nm) for amorphous Si barriers. Note that for the MgO barriers used here, two-step tunneling may also occur via oxygen vacancies as previously demonstrated [39].

IV. SUMMARY

The scaling of the proximity exchange field, which ferromagnetic Fe exerts on the spin accumulation at the MgO/Si interface of Fe/MgO/Si tunnel contacts, was investigated using the inverted Hanle effect. First, it was shown that the exchange field varies with the tunnel bias voltage in the same way as the square of the tunnel spin polarization. Second, it was found that the decay of the exchange field with increasing MgO thickness is rather weak and nonexponential. We argued that this is because the expected exponential decay is compensated by the improved epitaxial quality of the MgO, and the consequent enhancement of the spin-filtering properties at larger MgO thickness. After correcting for this, an exponential decay of the exchange field with t_{MgO} with a decay length of $\lambda = -0.42$ nm was obtained. Comparing this to the decay length for the tunnel conductance ($\lambda = -0.21$ nm) suggests that the exchange interaction is dominated by two-step tunneling processes.

[1] J. J. Hauser, Magnetic Proximity Effect, Phys. Rev. **187**, 580 (1969).

[2] F. Wilhelm, P. Poulopoulos, G. Ceballos, H. Wende, and K. Baberschke, P. Srivastava, D. Benea, H. Ebert, M. Angelakeris, N. K. Flevaris, D. Niarchos, A. Rogalev, N. B. Brookes, Layer-Resolved Magnetic Moments in Ni/Pt Multilayers, Phys. Rev. Lett. **85**, 413 (2000).

[3] I. Žutić, A. Matos-Abiague,B. Scharf, H. Dery, and K. Belashchenko, Proximitized materials, Mater. Today **22**, 85 (2019).

[4] P. Wei, S. Lee, F. Lemaitre, L. Pinel, D. Cutaia, W. Cha, F. Katmis, Y. Zhu, D. Heiman, J. Hone, J. S. Moodera, and C.-T. Chen, Strong interfacial exchange field in the graphene/EuS heterostructure, Nature Mater. **15**, 711 (2016).

[5] J. C. Leutenantsmeyer, A. A. Kaverzin, M. Wojtaszek, and B. J. van Wees, Proximity induced room temperature ferromagnetism in graphene probed with spin currents, 2D Mater. **4**, 014001 (2017).

[6] C. Zhao, T. Norden, P. Zhang, P. Zhao, Y. Cheng, F. Sun, J. P. Parry, P. Taheri, J. Wang, Y. Yang *et al.*, Enhanced valley splitting in monolayer WSe2 due to magnetic exchange field, Nat. Nanotechnol. **12**, 757 (2017).

[7] B. Karpiak, A. W. Cummings, K. Zollner, M. Vila, D. Khokhriakov, A. M. Hoque, A. Dankert, P. Svedlindh, J. Fabian, S. Roche, S. P. Dash, Magnetic proximity in a van der Waals heterostructure of magnetic insulator and graphene, 2D Mater. **7**, 015026 (2020).

[8] H. Haugen, D. Huertas-Hernando, and A. Brataas, Spin transport in proximity-induced ferromagnetic graphene, Phys. Rev. B **77**, 115406 (2008).

[9] Y. G. Semenov, K. W. Kim, and J. M. Zavada, Spin field effect transistor with a graphene channel, Appl. Phys. Lett. **91**, 153105 (2007).

[10] N. Tombros, C. Jozsa, M. Popinciuc, H. T. Jonkman, and B. J. van Wees, Electronic spin transport and spin precession in single graphene layers at room temperature, Nature (London) **448**, 571 (2007).

[11] W. Han, R. K. Kawakami, M. Gmitra, and J. Fabian, Graphene spintronics, Nat. Nanotechnol. **9**, 794 (2014).

[12] W. Han, Perspectives for spintronics in 2D materials, APL Mater. **4**, 032401 (2016).

[13] W. Yan, O. Txoperena, R. Llopis, H. Dery, L. E. Hueso, and F. Casanova, A two-dimensional spin field-effect switch, Nat. Commun. **7**, 13372 (2016).

[14] A. Dankert and S. P. Dash, Electrical gate control of spin current in van der Waals heterostructures at room temperature, Nat. Commun. **8**, 16093 (2017).

[15] J. C. Slonczewski, Conductance and exchange coupling of two ferromagnets separated by a tunneling barrier, Phys. Rev. B **39**, 6995 (1989).

[16] J. Faure-Vincent, C. Tiusan, C. Bellouard, E. Popova, M. Hehn, F. Montaigne, and A. Schuhl, Interlayer Magnetic Coupling Interactions of Two Ferromagnetic Layers by Spin Polarized Tunneling, Phys. Rev. Lett. **89**, 107206 (2002).

[17] T. Katayama, S. Yuasa, J. Velev, M. Ye. Zhuravlev, S. S. Jaswal, and E. Y. Tsymbal, Interlayer exchange coupling in Fe/MgO/Fe magnetic tunnel junctions, Appl. Phys. Lett. **89**, 112503 (2006).

[18] L. E. Nistor, B. Rodmacq, S. Auffret, A. Schuhl, M. Chshiev, and B. Dieny, Oscillatory interlayer exchange coupling in MgO tunnel junctions with perpendicular magnetic anisotropy, Phys. Rev. B **81**, 220407(R) (2010).

[19] Ł. Gladczuk, L. Gladczuk, P. Dluzewski, K. Lasek, P. Aleshkevych, D. M. Burn, G. van der Laan, and T. Hesjedal, Spin-current mediated exchange coupling in MgO-based magnetic tunnel junctions, Phys. Rev. B **103**, 064416 (2021).

[20] C. H. Du, H. L. Wang, Y. Pu, T. L. Meyer, P. M. Woodward, F. Y. Yang, and P. C. Hammel, Probing the Spin Pumping Mechanism: Exchange Coupling with Exponential Decay in $Y_3Fe_5O_{12}$/barrier/Pt Heterostructures, Phys. Rev. Lett. **111**, 247202 (2013).

[21] I. A. Akimov, M. Salewski, I. V. Kalitukha, S. V. Poltavtsev, J. Debus, D. Kudlacik, V. F. Sapega, N. E. Kopteva, E. Kirstein, E. A. Zhukov, D. R. Yakovlev, G. Karczewski, M. Wiater, T. Wojtowicz, V. L. Korenev, Y. G. Kusrayev, and M. Bayer, Direct measurement of the long-range p-d exchange coupling in a ferromagnet-semiconductor Co/CdMgTe/CdTe quantum well hybrid structure, Phys. Rev. B **96**, 184412 (2017).

[22] A. W. Cummings, Probing magnetism via spin dynamics in graphene/2D-ferromagnet heterostructures, J. Phys. Mater. **2**, 045007 (2019).

[23] I. Žutić, J. Fabian, and S. Das Sarma, Spintronics: fundamentals and applications, Rev. Mod. Phys. **76**, 323 (2004).

[24] J. Fabian, A. Matos-Abiague, C. Ertler, P. Stano, and I. Žutić, Semiconductor spintronics, Acta Physica Slovaca **57**, 565 (2007).

[25] R. Jansen, A. Spiesser, H. Saito, Y. Fujita, S. Yamada, K. Hamaya, and S. Yuasa, Proximity exchange coupling in a Fe/MgO/Si tunnel contact detected by the inverted Hanle effect, Phys. Rev. B **100**, 174432 (2019).

[26] R. Jansen, A. Spiesser, Y. Fujita, H. Saito, S. Yamada, K. Hamaya, and S. Yuasa, Proximity exchange coupling across an MgO tunnel barrier detected via spin precession, Proc. SPIE **11470**, 114700Z (2020).

[27] S. P. Dash, S. Sharma, J. C. Le Breton, J. Peiro, H. Jaffrès, J.-M. George, A. Lemaître, and R. Jansen, Spin precession and inverted Hanle effect in a semiconductor near a finite-roughness ferromagnetic interface, Phys. Rev. B **84**, 054410 (2011).

[28] A. Spiesser, H. Saito, Y. Fujita, S. Yamada, K. Hamaya, S. Yuasa, and R. Jansen, Giant Spin Accumulation in Silicon Nonlocal Spin-Transport Devices, Phys. Rev. Appl. **8**, 064023 (2017).

[29] R. Jansen, A. Spiesser, H. Saito, Y. Fujita, S. Yamada, K. Hamaya, and S. Yuasa, Nonlinear Electrical Spin Conversion in a Biased Ferromagnetic Tunnel Contact, Phys. Rev. Appl. **10**, 064050 (2018).

[30] A. Spiesser, H. Saito, S. Yuasa, and R. Jansen, Tunnel spin polarization of Fe/MgO/Si contacts reaching 90% with increasing MgO thickness, Phys. Rev. B **99**, 224427 (2019).

[31] X. Lou, C. Adelmann, M. Furis, S. A, Crooker, C. J. Palmstrøm, and P. A. Crowell, Electrical Detection of Spin Accumulation at a Ferromagnet-Semiconductor Interface, Phys. Rev. Lett. **96**, 176603 (2006).

[32] S. P. Dash, S. Sharma, R. S. Patel, M. P. de Jong, and R. Jansen, Electrical creation of spin polarization in silicon at room temperature, Nature (London) **462**, 491 (2009).

[33] K. Zollner, M. Gmitra, T. Frank, and J. Fabian, Theory of proximity-induced exchange coupling in graphene on hBN/(Co, Ni), Phys. Rev. B **94**, 155441 (2016).

[34] K. Zollner, P. E. Faria, Jr., and J. Fabian, Giant proximity exchange and valley splitting in transition metal dichalcogenide/hBN/(Co, Ni) heterostructures, Phys. Rev. B **101**, 085112 (2020).

[35] Y. Xu, D. Ephron and M. R. Beasley, Directed inelastic hopping of electrons through metal-insulator-metal tunnel junctions, Phys. Rev. B **52**, 2843 (1995).

[36] A. M. Bratkovsky, Tunneling of electrons in conventional and half-metallic systems: Towards very large magnetoresistance, Phys. Rev. B **56**, 2344 (1997).

[37] A. Vedyayev, D. Bagrets, A. Bagrets, and B. Dieny, Resonant spin-dependent tunneling in spin-valve junctions in the presence of paramagnetic impurities, Phys. Rev. B **63**, 064429 (2001).

[38] M. Y. Zhuravlev, E. Y. Tsymbal, and A. V. Vedyayev, Impurity-Assisted Interlayer Exchange Coupling across a Tunnel Barrier, Phys. Rev. Lett. **94**, 026806 (2005).

[39] G. X. Miao, Y. J. Park, J. S. Moodera, M. Seibt, G. Eilers, and M. Münzenberg, Disturbance of Tunneling Coherence by Oxygen Vacancy in Epitaxial Fe/MgO/Fe Magnetic Tunnel Junctions, Phys. Rev. Lett. **100**, 246803 (2008).